

1 Navigated ultrasound bronchoscopy with integrated 2 positron emission tomography - A human feasibility study

3 Arne Kildahl-Andersen^{1,2,3}, Erlend Fagertun Hofstad⁴, Ole-Vegard Solberg⁴,
4 Hanne Sorger^{2,5}, Tore Amundsen^{1,2}, Thomas Langø^{3,4}, Håkon Olav Leira^{1,2}

5 *¹Department of Thoracic Medicine, St. Olavs hospital, Trondheim University Hospital,*

6 *Postboks 3250, Sluppen, 7006 Trondheim, Norway*

7 *²Department of Circulation and Medical Imaging, Faculty of Medicine, Norwegian*

8 *University of Science and Technology (NTNU), AHL-senteret, Prinsesse Kristinas gate 3,*

9 *Trondheim, Norway*

10 *³Department of Research, St. Olavs hospital, Trondheim University Hospital, Postboks 3250,*

11 *Sluppen, 7006 Trondheim, Norway*

12 *⁴Department of Health Research, SINTEF Digital, Postboks 4760 Torgarden, 7465*

13 *Trondheim, Norway*

14 *⁵Department of Medicine, Levanger Hospital, Nord-Trøndelag Hospital Trust, Levanger,*

15 *Norway*

16

17 Corresponding author:

18 Arne Kildahl-Andersen

19 Department of Thoracic Medicine

20 St. Olavs hospital, Trondheim University Hospital

21 Postboks 3250 Sluppen

22 NO 7006 Trondheim

23 Norway

24 Email: arne.kildahl-andersen@ntnu.no

25

NOTE: This preprint reports new research that has not been certified by peer review and should not be used to guide clinical practice.

26

27 **Abstract**

28 *Background and objective:* Patients suspected to have lung cancer, undergo endobronchial
29 ultrasound bronchoscopy (EBUS) for the purpose of diagnosis and staging. For presumptive
30 curable patients, the EBUS bronchoscopy is planned based on images and data from
31 computed tomography (CT) images and positron emission tomography (PET). Our study
32 aimed to evaluate the feasibility of a multimodal electromagnetic navigation platform for
33 EBUS bronchoscopy, integrating ultrasound and segmented CT, and PET scan imaging data.

34 *Methods:* The proof-of-concept study included patients with suspected lung cancer and
35 pathological mediastinal/hilar lymph nodes identified on both CT and PET scans. Images
36 obtained from these two modalities were segmented to delineate target lymph nodes and then
37 incorporated into the CustusX navigation platform. The EBUS bronchoscope was equipped
38 with a sensor, calibrated, and affixed to a 3D printed click-on device positioned at the
39 bronchoscope's tip. Navigation accuracy was measured postoperatively using ultrasound
40 recordings.

41 *Results:* The study enrolled three patients, all presenting with suspected mediastinal lymph
42 node metastasis (N1-3). All PET-positive lymph nodes were displayed in the navigation
43 platform during the EBUS procedures. In total, five distinct lymph nodes were sampled,
44 yielding malignant cells from three nodes and lymphocytes from the remaining two. The
45 median accuracy of the navigation system was 7.7 mm.

46 *Conclusion:* Our study introduces a feasible multimodal electromagnetic navigation platform
47 that combines intraoperative ultrasound with preoperative segmented CT and PET imaging
48 data for EBUS lymph node staging examinations. This innovative approach holds promise for
49 enhancing the accuracy and effectiveness of EBUS procedures.

50

51 **Keywords:** *Electromagnetic navigation, Endobronchial ultrasound, Convex probe*
52 *endobronchial ultrasound, Navigated EBUS, Positron emission tomography*

53

54 **Introduction**

55 Lung cancer stands as a leading cause of cancer-related death worldwide with a 18% of all
56 cancer-fatalities in 2020 [1]. Early detection and efficient work-up is crucial for a favourable
57 prognosis, as lung cancer is curable at an early stage. To identify patients eligible for curative
58 treatment imaging with computed tomography (CT) followed by 18F-fluorodeoxyglucose
59 (FDG) positron emission tomography (PET) scan is needed. These examinations form the
60 basis for a clinical TNM staging, which describes size and features of the primary tumor (T),
61 as well as involvement of hilar and mediastinal nodes (N) and the presence of distant
62 metastasis (M). Subsequently, the radiological findings must be confirmed by invasive
63 sampling, providing both a diagnosis and accurate staging information.

64 Endobronchial ultrasound bronchoscopy (EBUS) is the state-of-the-art tissue
65 examination of PET-positive and/or enlarged lymph nodes (N-stage) within the lung hilus and
66 mediastinum. Moreover, comprehensive mediastinal and hilar EBUS screening is strongly
67 advised in scenarios involving tumors larger than 3 cm, central tumors, and cases with
68 radiological N1-involvement [2]. This recommendation stems from the recognition that PET-
69 CT scans, especially those indicating only hilar lymph node involvement (N1) or
70 demonstrating a negative lymph node status (N0), may occasionally yield false negatives. An
71 EBUS upstaging of 6% is shown in an observational study of Naur et al in such cases [3].

72 Bronchoscope with convex EBUS (CP-EBUS) probe enables real-time visualized or
73 guided transbronchial needle aspirations (TBNA). Current lung cancer guidelines recommend
74 sampling lymph nodes down to 5 mm in short axis when treatment to cure is intended [4]. At
75 least three repeated needle aspirations are recommended for diagnosing lung cancer without

76 rapid onsite evaluations (ROSE), even more to ensure an ample quantity of material for
77 subsequent immunohistochemical and mutational analysis [4]. Notably, a study by Lee et al
78 demonstrates that three needle aspirations exhibit a negative predictive value of 97%, proving
79 effective in ruling out malignant involvement of a lymph node [5]. Assessment of hilar or
80 mediastinal lymph node in lung cancer work-up with EBUS TBNA has shown specificity and
81 sensitivity > 90% in meta-analysis [6, 7]. Additional procedures like elastography and ROSE
82 have not contributed to higher sensitivity [8].

83 Limitations of EBUS include dependence on operator experience and individual learning
84 curves, as evident in several studies [9-11]. The bronchoscopist must comprehend the
85 mediastinal anatomy and possess a well-trained ability to mentally visualize preprocedural CT
86 scans in three dimensions. To locate a specific lymph node station the initial navigation is
87 mainly video-dependent. Subsequently, ultrasound localization of the lymph node(s) follows,
88 presenting challenges such as a limited 60° ultrasound scan sector and occasional suboptimal
89 images due to ultrasound artifacts and variable probe-to-wall contact. Furthermore, the ability
90 to perform repeated aspirations on the same lymph node is crucial for obtaining representative
91 samples. However, lymph node relocation becomes challenging after each aspiration, as the
92 video view is often obscured by blood and mucus.

93 Electromagnetic navigation (EM) bronchoscopy (ENB) was first demonstrated
94 successfully in humans in a study of Schwarz et al in 2006 [12]. Since then, ENB has been a
95 growing field of research for diagnosing lung lesions located beyond visual access in the
96 periphery of the lungs. However, Sorger et al has presented a system for ENB suitable for
97 diagnosing mediastinal/hilar lymph nodes accessible for CP-EBUS [13, 14]. The clinical
98 rationale behind incorporating ENB with EBUS lies in addressing the challenges associated
99 with video dependency. In this study, the tracking sensor were permanently fixated to the
100 EBUS bronchoscope with glue and endoscopy rubber wrap. Not confined to one EBUS

101 bronchoscope, a single-use 3D printed click-on device to attach the EM tracking sensor was
102 developed [15]. However, this click-on device has never been tested with ENB in patients.

103 Our study introduces novel features as the fixation click-on device for EM tracking
104 sensor including a preoperative tracking sensor-to-ultrasound image calibration procedure.
105 Methods for CT segmentations are implemented and a real-time integration of PET-CT data
106 during EBUS bronchoscopy is introduced, allowing for the identification of PET-positive
107 lymph nodes during ENB. Our study aimed to evaluate the feasibility of a complete
108 multimodal image guidance platform for navigated CP-EBUS in humans.

109

110

111 **Material and methods**

112 **Study design and patients**

113 The study was designed as a non-randomized proof-of-concept study with patients recruited
114 prospectively. Inclusion criteria were patients > 18 years, non-pregnant, and referred to the
115 thoracic department with suspected lung cancer and possible curable disease. Patients eligible
116 for participation exhibited pathological mediastinal or hilar lymph nodes warranting a PET-
117 CT examination. The study was approved by the regional ethics committee (ID 13136), being
118 in accordance with the Declaration of Helsinki. Written and informed consent was collected
119 from the patients. The patients were included from August to October 2023.

120

121 **Electromagnetic navigation platform**

122 The ENB system is constructed upon the open-source navigation research platform, CustusX
123 [16]. The preoperative and intraoperative setup steps of the ENB system are illustrated in
124 Figure 1. Preoperative radiologic imaging data underwent automated airway segmentation

125 processes [17], and artificial intelligence (AI)-based segmentation of lymph nodes and vessels
126 [18]. Image-to-patient registration was performed by automated airway centerline estimations
127 of the tracked EBUS bronchoscope's positions during the initial phase of the procedure [19].
128 The tracking sensor was affixed to the distal end of the EBUS bronchoscope using a 3D
129 printed clip-on device made of Ultem™ 1010 resin developed in our research group. The
130 disposable clip-on device has been tested previously on a healthy volunteer [15]. A quick on-
131 site EM tracking-to-ultrasound calibration was performed using a probe calibration adapter
132 [15]. During the bronchoscopy, CustusX displays a combination of preoperative and real-time
133 intraoperative images. A graphical user interface with both video, ultrasound, virtual
134 bronchoscopy, or CT could then be obtained. Finally, by combining different image
135 modalities with EM tracking a navigation map is presented for the bronchoscopist in real-time
136 to guide the procedure.

137

138 **Fig 1. The steps of image preprocessing and EBUS bronchoscope modifications that**
139 **enables electromagnetic navigation bronchoscopy (ENB).** Airways and lymph nodes are
140 segmented from the CT images and registered to PET. An electromagnetic (EM) sensor is
141 fixated to the EBUS bronchoscope and calibrated to the ultrasound scan sector with a 3D-
142 printed adapter. Intraoperatively the CT/PET images are registered to the patient, before
143 enabling the bronchoscopist to navigate to the target supported by ENB and ultrasound

144

145 **Equipment for bronchoscopy electromagnetic position tracking**
146 **system**

147 CP-EBUS (Olympus BF-UC180F, Olympus, Tokyo, Japan)

- 148 Video processing unit (Olympus, Evis Excera III CV-190 Plus, Olympus, Tokyo,
- 149 Japan)
- 150 Light source (Olympus, Evis Excera III CLV-190, Olympus, Tokyo, Japan)
- 151 Ultrasound processor (Olympus EVIS EUS EU-ME2, Olympus, Tokyo, Japan)
- 152 CustusX (In-house developed open-source research system for image guiding and
- 153 navigation, www.custusx.org) [16]
- 154 Aurora[®] electromagnetic tracking system (Northern Digital Inc. (NDI), Waterloo, ON,
- 155 Canada)
- 156 Tracking sensor (Aurora 6-DOF Probe, Straight Tip, Standard, Northern Digital Inc.,
- 157 Waterloo, ON, Canada)
- 158 3D printed clip-on device made in Ultem[™] for attaching the electromagnetic tracking
- 159 sensor to the bronchoscope [15]
- 160 3D printed EBUS bronchoscope adapter for calibration [15]

161 **Integrating PET-CT imaging data into the navigation platform**

162 Patients included in the study underwent a PET-CT scan as part of the staging process for
163 suspected lung cancer. However, the lowdose CT scan acquired simultaneously to merge
164 with the PET tracer imaging data has limited resolution and is without intravenous contrast.
165 To enhance the precision of the imaging, a high-resolution thorax CT scan with a slice
166 thickness of 1 mm, conducted weeks before the PET examination, was registered to the
167 lowdose PET-CT data. This registration process involved a 3-D deformable registration,
168 necessary as the PET imaging data was captured during different respiratory phases compared
169 to the initial high-resolution CT. The Elastix toolbox was integrated into CustusX for this
170 purpose [20, 21].

171

172 **Technical and clinical outcomes**

173 Navigation accuracies were measured postoperatively. This involved a manual operation
174 using both lymph nodes and large vessels displayed on the ultrasound recordings as gold
175 standard. The positions of these structures were then compared to their counterparts in the
176 segmented 3-D CT map. The total procedure time of the EBUS examinations was recorded.
177 The TBNA were carried out without deviation from routine clinical practice, where the
178 primary outcome was to successfully achieve a diagnosis from each sampled lymph node. The
179 3D printed clip-on device with EM sensor was qualitatively evaluated by inspection after each
180 procedure to determine if it remained robustly attached to the CP-EBUS.

181

182

183 **Results**

184 Included in the study were two female and one male referred to the department of thoracic
185 medicine due to symptoms of suspected lung cancer. The CT and PET imaging data were
186 segmented and displayed intraoperatively. Segmented images rendered on the navigation
187 platform are shown alongside ultrasound in Figs 2 to 4. All lymph nodes were correctly
188 segmented, with the exception of one PET-negative station 7 node from patient 1. The
189 timespan separating high-resolution CT and PET-CT to EBUS ranged from 16 to 29 days and
190 6 to 10 days, respectively. After PET-CT patient 3 had questionable distant lymph node
191 spread to left thigh (not puncturable). The TNM-stage of the patients is shown in Table 1.

192

193 **Fig 2. Graphical renderings from patient 1 as displayed on the navigation platform. In**
194 **the 3D renderings on the left (A), the ultrasound scan sector showing lymph node station 11R.**
195 **A lung tumor in the upper lobe of the left lung is highlighted in yellow, indicative of PET**

196 positivity, while the lymph nodes are depicted in green, signifying PET negativity. The top
197 right (B) displays the ultrasound view from the EBUS bronchoscope, and in the lower right
198 (C), the EBUS bronchoscope's probe and ultrasound scan sector is visualized together with
199 the CT images and overlaid the segmented lymph node (green).

200

201 **Fig 3. Segmented 3D CT renderings, patient 2.** Great thoracic vessels displayed
202 intraoperatively, with the ultrasound scan sector showing the left subclavian artery (*).

203

204 **Fig 4. Graphical user interface during sampling, patient 3.** In the segmented 3D CT and
205 PET-CT renderings (A), the EBUS probe is shown during needle aspirations of lymph node
206 station 10R. The top right (B) illustrates the ultrasound view from the bronchoscope, showing
207 both the needle and a relatively large lymph node. The lymph node, identified as PET-
208 positive, thereby displayed in red in both the hybrid PET-CT-ultrasound image (C) and the
209 3D PET-CT renderings (A).

210

211 The EBUS bronchoscopy procedures lasted between 20 to 25 minutes for all three
212 patients. Except for the initial registration of the preoperative CT data to the patient,
213 procedures were not impeded by the additional equipment. Rapid onsite examination (ROSE)
214 was only employed for patient 3. Malignant cells were found in the sampled lymph node
215 stations in two of the three patients. In the first patient, EBUS sampling results revealed
216 lymphoid cells, but squamous cell carcinoma (SCC) was diagnosed with four forceps biopsies
217 from the primary tumor. Detailed results from imaging and EBUS examinations are provided
218 in Table 1.

219 **Table 1. Three patients examined with navigated EBUS: Technical outcomes**

Patient	Stage (TNM)	Primary tumor size (mm)	LN stations	Size[§] (mm)	Median accuracy (mm)	Range (mm)	Aspirations	Diagnosis	Duration (min)
1	cT4N2M0	114	7	9	NA	NA	3	LC	20
			11R	10	8.3	3.9-13.3	4	LC	
2	cT4N3M0	89	2R	16	8.3	7.9-10.5	4	NSCLC	23
			4R	8	7.0	6.7-7.2	4	NSCLC	
3	cT1cN1(3)M1b	18	10R	20	3.5	3.1-6.8	5	NSCLC	25

220 The table shows sampled lymph node (LN) stations, size (from CT scan), median accuracy for each station and number of needle
 221 aspirations(passes). In addition to a NSCLC diagnosis, the provided cytologies from patient 2 showed anaplastic lymphoma kinase (ALK)
 222 positive cancer.

223 § CT scan lymph node size in short axis

224 LC= Lymphoid cells, NSCLC=Non-small cell lung cancer

225 The 3D printed clip-on device affixed at the tip of the EBUS bronchoscopy remained
226 securely attached throughout the examinations. Importantly, all bronchoscopies were
227 performed without complications for the patients, demonstrating no excess bleeding,
228 pneumothorax, or post-procedure infections.

229 The navigation accuracies for the three patients were measured postoperatively and were
230 assessed by analyzing image recordings from the navigation platform. A total of 24 target
231 points, sampled from ten distinct anatomical locations, were included in the measurements.

232 Given that ultrasound 3D acquisitions were beyond the scope of this study, the measurements
233 were confined to 2D ultrasound images. To mitigate bias, measurements were systematically
234 taken from various scan sector directions.

235 Median accuracy estimated from the ten anatomical positions was 7.7 mm, and range was 3.3-
236 15.3 mm.

237

238 **Discussion**

239 This proof-of-concept study establishes the feasibility of a multimodal ENB platform for the
240 staging of mediastinal and hilar lymph nodes in lung cancer. The platform integrates
241 multimodal and elastic co-registration of images (CT and PET), EBUS, and AI-based
242 segmentation of central airways, vessels, and lymph node. The final result is a multimode
243 ENB, PET CT, and EBUS guiding platform for the mediastinal/hilar lymph nodes. By adding
244 PET-CT to the ENB platform the bronchoscopist is able to discern between PET positive and
245 negative lymph nodes in real-time. This is a useful feature to guide sampling, especially in
246 cases where PET positive and negative lymph nodes coexist in the same lymph node station.

247 The median accuracy of 7.7 mm compares well with findings from prior articles on
248 similar subject [14, 22]. Notably, the measured accuracy appears reasonable when considering

249 a preliminary phantom study involving the current click-on device and preprocedural
250 calibration system, demonstrating an accuracy of 3.9 mm [15]. In a previous study utilizing
251 the CustusX navigation platform, Sorger et al reported an overall accuracy of 10.0 mm in
252 examining four patients [14]. Other studies utilizing ENB for peripheral lung tumors have
253 indicated navigation accuracy ranging from 5.7 to 9.0 mm [22]. When utilizing ENB on
254 humans, additional offset values are introduced due to cardiorespiratory movements and
255 displacement of lung tissue by the ultrasound probe pushing the bronchial wall [23]. Our
256 study indicates a greater impact on navigation accuracy errors in the hilus region, specifically
257 at station 11, as this area is more susceptible to respiratory movements and probe induced
258 displacements than stations situated along the trachea [23]. This accuracy error becomes
259 more clinically relevant in the clinical context of transbronchial sampling of peripheral lung
260 tumors without real-time ultrasound guidance.

261 A virtual EBUS bronchoscopy that enables preoperative planning and
262 intraoperative guidance of bronchial wall puncture sites was presented in a study of Sato et al
263 [24]. A virtual EBUS was performed first to determine puncture spots and angles, followed by
264 a real EBUS examination of the patient performed based upon this information. In contrast,
265 our system offers instantaneous EBUS to CT localization within the airways, presenting a
266 valuable advantage. Addressing a practical concern with traditional EBUS bronchoscopy,
267 where mucus or blood can obscure the bronchoscope video during needle aspirations, EM
268 navigation virtual bronchoscopy (from 3D CT), can be used independent from the real video.
269 Ensuring repeated needle aspirations come from the same lymph node is crucial for
270 bronchoscopists. ENB facilitates swift relocation to the same lymph node when repeated
271 aspirations are necessary, potentially optimizing procedure duration. Finally, adding ENB to
272 EBUS will grant navigational assurance for the novice bronchoscopists unfamiliar to EBUS,

273 as it displays the bronchoscope's anatomical 3D position relative to the mediastinal and hilar
274 anatomy.

275 The studies of Zang et al outline a system combining virtual video bronchoscopy and
276 CT-based virtual EBUS registered to real EBUS [25, 26]. The proposed method combines
277 segmentation of both ultrasound and CT images that are fused through a six-step algorithm
278 based on mutual information and region shape information. The method has advantages such
279 as not requiring extra sensors or navigation hardware, but segmentation of nodal regions of
280 interest (ROI) was time-consuming. As often is the case, many lymph nodes are to be
281 examined, so that total segmentation time could be perceived disruptive in a EBUS workflow,
282 especially when patients are under conscious sedation. Despite this, both navigation systems,
283 including ours, prove beneficial for learning purposes for novice EBUS bronchoscopists,
284 addressing the challenging learning curve associated with EBUS.

285 Compared to a software-only solution, a complete EM platform setup with
286 calibration and registration to patients is more complex and time consuming. Inherent
287 navigation accuracy errors, metallic hardware interference, registration errors, and
288 cardiorespiratory motions contribute to CT-to-body divergence. However, ENB systems have
289 demonstrated efficacy in diagnosing peripheral lung nodules [27]. In clinical scenarios with
290 both peripheral tumors and enlarged mediastinal lymph nodes, using ENB for navigation to
291 both sites during the same session is justifiable. Nonetheless, ENB competes with alternative
292 techniques, like tomosynthesis and robotics [28], and its future role, especially in the lung
293 periphery, remains to be determined [29].

294 Our study limitations include the small number of participants and the introduction of
295 a 3D printed clip-on device, which, though complication-free in our study, could pose
296 potential issues. Future considerations may involve tracking cytology needles
297 electromagnetically, eliminating the need for externally attached sensors. Segmentation of one

298 of the lymph nodes failed, showing that manual verification before bronchoscopy remains
299 essential. Finally, the postprocedural measurements were limited to only two orthogonal
300 planes in the 2D ultrasound scan sector. Though, by measuring accuracy from different
301 anatomical sites and ultrasound scan directions we aimed at lowering the likelihood of bias in
302 the navigation accuracy measurements.

303 Diagnostic yield and procedural time reduction could be potential benefits of
304 navigation platforms, which could be explored in future trials. The intraoperative captured
305 multimodal images could serve as quality indicators and documentations that could be
306 reviewed on multi-disciplinary meetings. Our ongoing research explores machine learning for
307 recognizing specific lymph node stations during EBUS bronchoscopy, with ENB serving as a
308 golden standard linking patient anatomy from CT to intraoperative video and ultrasound
309 recordings.

310 In conclusion, our study demonstrates the feasibility of integrating PET imaging data
311 into a multimodal EM navigation platform for lymph node staging examinations. Introducing
312 PET data during real-time EBUS provides valuable information for prioritizing invasive
313 sampling. Future trials and advancements, including further image analytics with machine
314 learning, will unveil the full potential of navigation platforms in enhancing bronchoscopy
315 procedures.

316

317 **Acknowledgements:**

318 We thank Marit Setvik and Solfrid Meier Løwensprung, Department of Thoracic Medicine, St. Olavs
319 hospital, for their contribution in assisting the bronchoscopy. This work was supported by St. Olavs
320 hospital, the Liaison Committee for Education, Research and Innovation in Central Norway and
321 SINTEF Research group for Medical Technology, the Ministry of Health, and Social Affairs of
322 Norway through the Norwegian National Advisory Unit for Ultrasound an Image-Guided Therapy (St.
323 Olavs hospital, Trondheim, Norway)

324 **References**

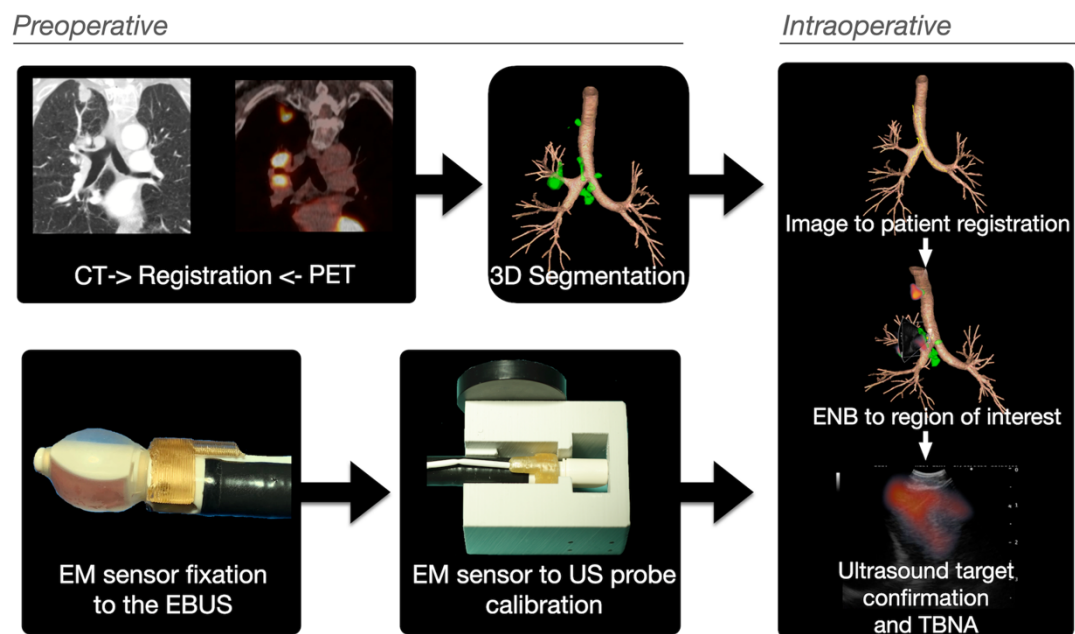
- 325 1. Sung H, Ferlay J, Siegel RL, Laversanne M, Soerjomataram I, Jemal A, et al. Global
326 Cancer Statistics 2020: GLOBOCAN Estimates of Incidence and Mortality
327 Worldwide for 36 Cancers in 185 Countries. *CA: Cancer. J. Clin.* 2021; 71: 209-49.
- 328 2. Postmus PE, Kerr KM, Oudkerk M, Senan S, Waller DA, Vansteenkiste J, et al. Early
329 and locally advanced non-small-cell lung cancer (NSCLC): ESMO Clinical Practice
330 Guidelines for diagnosis, treatment and follow-up. *Ann. Oncol.* 2017; 28 (suppl 4):
331 iv1-iv21.
- 332 3. Naur TMH, Konge L, Clementsen PF. Endobronchial Ultrasound-Guided
333 Transbronchial Needle Aspiration for Staging of Patients with Non-Small Cell Lung
334 Cancer without Mediastinal Involvement at Positron Emission Tomography-
335 Computed Tomography. *Respiration* 2017; 94: 279-84.
- 336 4. Wahidi MM, Herth F, Yasufuku K, Shepherd RW, Yarmus L, Chawla M, et al.
337 Technical Aspects of Endobronchial Ultrasound-Guided Transbronchial Needle
338 Aspiration: CHEST Guideline and Expert Panel Report. *Chest* 2016; 149: 816-35.
- 339 5. Lee HS, Lee GK, Lee HS, Kim MS, Lee JM, Kim HY, et al. Real-time endobronchial
340 ultrasound-guided transbronchial needle aspiration in mediastinal staging of non-small
341 cell lung cancer: how many aspirations per target lymph node station? *Chest* 2008;
342 134: 368-74.
- 343 6. Gu P, Zhao YZ, Jiang LY, Zhang W, Xin Y, Han BH. Endobronchial ultrasound-
344 guided transbronchial needle aspiration for staging of lung cancer: a systematic review
345 and meta-analysis. *Eur. J. Cancer* 2009; 45: 1389-96.
- 346 7. Adams K, Shah PL, Edmonds L, Lim E. Test performance of endobronchial
347 ultrasound and transbronchial needle aspiration biopsy for mediastinal staging in

- 348 patients with lung cancer: systematic review and meta-analysis. *Thorax* 2009; 64: 757-
349 62.
- 350 8. Sehgal IS, Dhooria S, Aggarwal AN, Agarwal R. Impact of Rapid On-Site Cytological
351 Evaluation (ROSE) on the Diagnostic Yield of Transbronchial Needle Aspiration
352 During Mediastinal Lymph Node Sampling: Systematic Review and Meta-Analysis.
353 *Chest* 2018; 153: 929-38.
- 354 9. Fusco L, Varone F, Magnini D, Pecoriello A, Montemurro G, Angeletti G, et al.
355 Influence of the Learning Effect on the Diagnostic Yield of Endobronchial
356 Ultrasound-guided Transbronchial Needle Aspiration of Mediastinal and Hilar Lymph
357 Nodes. *J. Bronchol. Intervent. Pulmonol.* 2017; 24: 193-9.
- 358 10. Flandes J, Giraldo-Cadavid LF, Perez-Warnisher MT, Gimenez A, Fernandez-
359 Navamuel I, Alfayate J, et al. Learning curves and association of pathologist's
360 performance with the diagnostic accuracy of linear endobronchial ultrasound
361 transbronchial needle aspiration (EBUS-TBNA): a cohort study in a tertiary care
362 reference centre. *BMJ Open* 2022; 12: e051257.
- 363 11. Sorhaug S, Hjelde H, Hatlen P, Leira HO, Salarinejad M, Nesvik B, et al. Learning
364 endobronchial ultrasound transbronchial needle aspiration - a 6-year experience at a
365 single institution. *Clin. Respir. J.* 2018; 12: 40-7.
- 366 12. Schwarz Y, Greif J, Becker HD, Ernst A, Mehta A. Real-time electromagnetic
367 navigation bronchoscopy to peripheral lung lesions using overlaid CT images: the first
368 human study. *Chest* 2006; 129: 988-94.
- 369 13. Sorger H, Hofstad EF, Amundsen T, Lango T, Leira HO. A novel platform for
370 electromagnetic navigated ultrasound bronchoscopy (EBUS). *Int. J. Comput. Assist.*
371 *Radiol. Surg.* 2016; 11: 1431-43.

- 372 14. Sorger H, Hofstad EF, Amundsen T, Lango T, Bakeng JB, Leira HO. A multimodal
373 image guiding system for Navigated Ultrasound Bronchoscopy (EBUS): A human
374 feasibility study. *PLoS One* 2017; 12: e0171841.
- 375 15. Kildahl-Andersen A, Hofstad EF, Peters K, Van Beek G, Sorger H, Amundsen T, et
376 al. A novel clip-on device for electromagnetic tracking in endobronchial ultrasound
377 bronchoscopy. *Minim. Invasive. Ther. Allied Technol.* 2022; 31:1041-9.
- 378 16. Askeland C, Solberg OV, Bakeng JB, Reinertsen I, Tangen GA, Hofstad EF, et al.
379 CustusX: an open-source research platform for image-guided therapy. *Int. J. Comput.*
380 *Assist. Radiol. Surg.* 2016; 11: 505-19.
- 381 17. Stoverud KH, Bouget D, Pedersen A, Leira HO, Lango T, Hofstad EF. *Aeropath: An*
382 *airway segmentation benchmark dataset with challenging pathology.* *ArXiv* 2023:
383 <https://doi.org/10.48550/arXiv.2311.01138>.
- 384 18. Bouget D, Jorgensen A, Kiss G, Leira HO, Lango T. Semantic segmentation and
385 detection of mediastinal lymph nodes and anatomical structures in CT data for lung
386 cancer staging. *Int. J. Comput. Assist. Radiol. Surg.* 2019; 14: 977-86.
- 387 19. Hofstad EF, Sorger H, Leira HO, Amundsen T, Lango T. Automatic registration of CT
388 images to patient during the initial phase of bronchoscopy: a clinical pilot study. *Med.*
389 *Phys.* 2014; 41: 041903.
- 390 20. Shamonin DP, Bron EE, Lelieveldt BP, Smits M, Klein S, Staring M, et al. Fast
391 parallel image registration on CPU and GPU for diagnostic classification of
392 Alzheimer's disease. *Front. Neuroinform.* 2013; 7: 50.
- 393 21. Klein S, Staring M, Murphy K, Viergever MA, Pluim JP. elastix: a toolbox for
394 intensity-based medical image registration. *IEEE Trans. Med. Imaging.* 2010; 29: 196-
395 205.

- 396 22. Eberhardt R, Anantham D, Herth F, Feller-Kopman D, Ernst A. Electromagnetic
397 navigation diagnostic bronchoscopy in peripheral lung lesions. *Chest* 2007; 131: 1800-
398 5.
- 399 23. Leira HO, Lango T, Sorger H, Hofstad EF, Amundsen T. Bronchoscope-induced
400 displacement of lung targets: first in vivo demonstration of effect from wedging
401 maneuver in navigated bronchoscopy. *J. Bronchol. Intervent. Pulmonol.* 2013; 20:
402 206-12.
- 403 24. Sato M, Chen F, Aoyama A, Yamada T, Ikeda M, Bando T, et al. Virtual
404 endobronchial ultrasound for transbronchial needle aspiration. *J. Thorac. Cardiovasc.*
405 *Surg.* 2013; 146: 1204-12.
- 406 25. Zang X, Zhao W, Toth J, Bascom R, Higgins W. Multimodal Registration for Image-
407 Guided EBUS Bronchoscopy. *J. Imaging* 2022; 8: 189.
- 408 26. Zang X, Cheirsilp R, Byrnes PD, Kuhlengel TK, Abendroth C, Allen T, et al. Image-
409 guided EBUS bronchoscopy system for lung-cancer staging. *Inform. Med. Unlocked*
410 2021; 25: 100665.
- 411 27. Folch EE, Pritchett MA, Nead MA, Bowling MR, Murgu SD, Krimsky WS, et al.
412 Electromagnetic Navigation Bronchoscopy for Peripheral Pulmonary Lesions: One-
413 Year Results of the Prospective, Multicenter NAVIGATE Study. *J. Thorac. Oncol.*
414 2019; 14: 445-58.
- 415 28. Kops SEP, Heus P, Korevaar DA, Damen JAA, Idema DL, Verhoeven RLJ, et al.
416 Diagnostic yield and safety of navigation bronchoscopy: A systematic review and
417 meta-analysis. *Lung Cancer.* 2023; 180: 107196.
- 418 29. Shaller BD, Gildea TR. What is the value of electromagnetic navigation in lung cancer
419 and to what extent does it require improvement? *Expert Rev. Respir. Med.* 2020;14:
420 655-69.

421 Figure 1

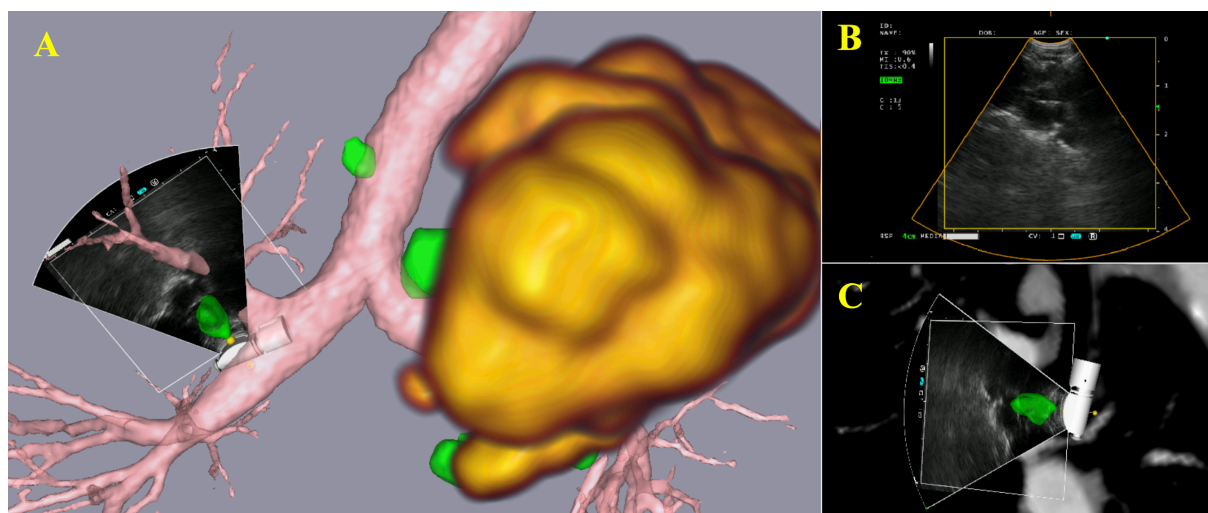


422

423

424

425 Figure 2



426

427

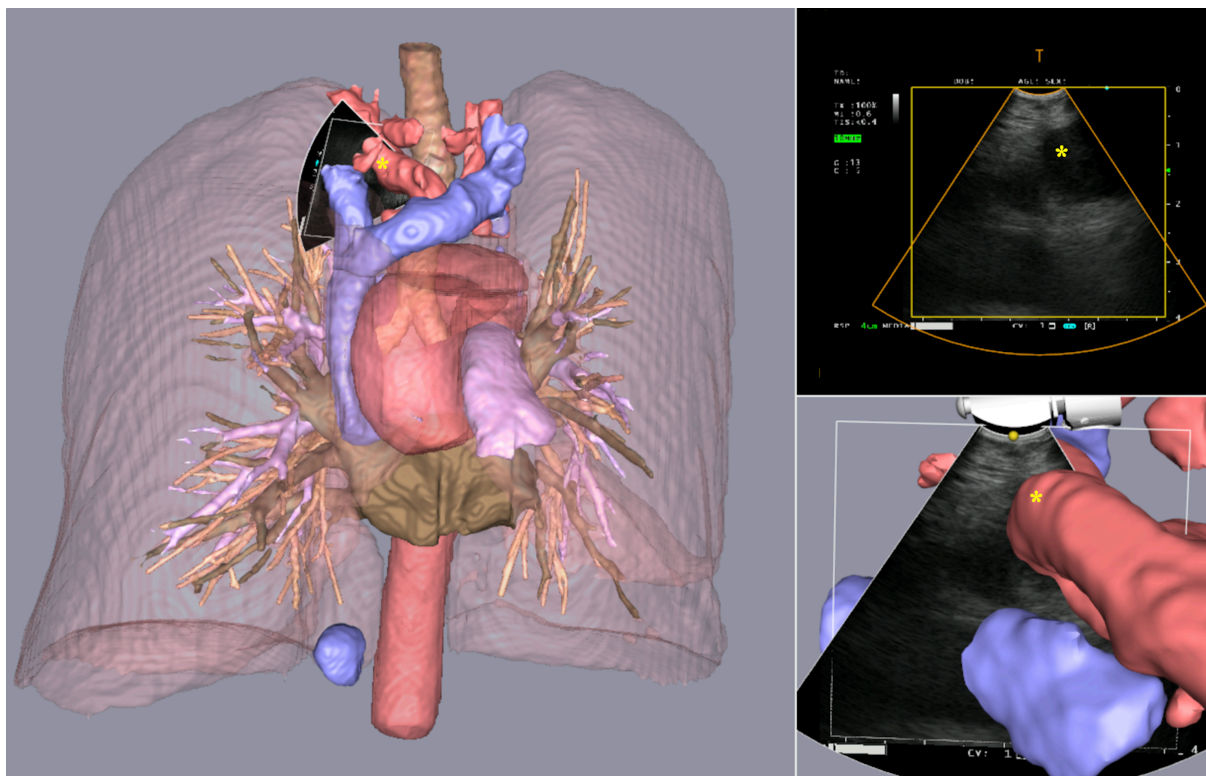
428

429

430

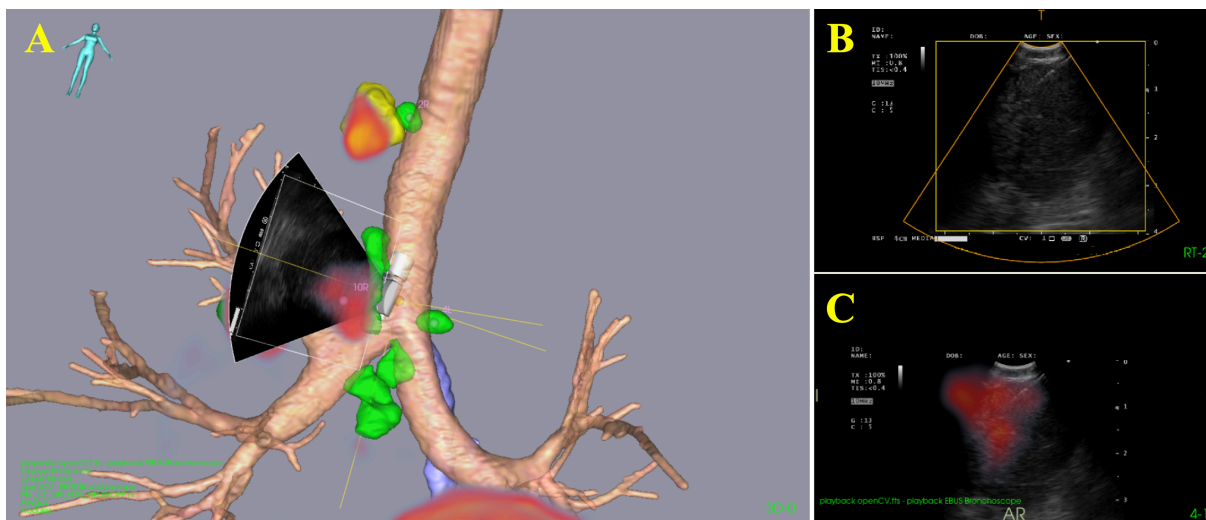
431
432
433

Figure 3



434
435
436
437
438

Figure 4



439
440
441
442
443
444

